Nilay Gizli

MORPHOLOGICAL CHARACTERIZATION OF CELLULOSE ACETATE BASED REVERSE OSMOSIS MEMBRANES BY ATOMIC FORCE MICROSCOPY (AFM)   EFFECT OF EVAPORATION TIME

Department of Chemical Engineering, Ege University, Bornova, 35100 İzmir, Turkey

Abstract. The surface structures of asymmetric cellulose acetate membranes prepared by the phase inversion method were investigated by the atomic force microscopy (AFM). The differences in the surface morphology have been expressed in terms of four types of roughness parameters such as; roughness average (S_a), root mean square roughness (S_q), surface skewness (S_{sk}), and surface kurtosis (S_{ku}). The association of the roughness characteristics with the salt rejection performance has also been investigated. The results show that the increase in the evaporation time, results in the change of the membrane morphology and rejection efficiency.

Keywords: atomic force microscopy, reverse osmosis membrane, morphology, surface roughness.

1. Introduction

Atomic Force Microscopy (AFM) gives the topographic images in 3D by scanning with a sharp tip over a surface. It is a useful method to characterize the surface structures of membranes due to the possibility of analyzing dry or wet samples without any special pretreatment. AFM imaging of the membrane structure has advantages over both the scanning electron microscopy (SEM) and transmission electron microscopy (TEM). Since the resolution is higher, the sample preparation is minimum and no electron beam damage occurs [1, 2]. In addition to its imaging capability, AFM can measure the interaction forces which allow the characterization of the adhesive behavior of a polymer film in the nanoscale level. Hence, AFM has become a popular method of investigating the surface structures of polymer and inorganic membranes. AFM characterization of a membrane has been focused on the determination of the surface morphology and pore structures (pore size, pore size distribution, pore density, surface roughness) [3-10], correlation of the membrane structure with membrane properties [1, 11-14], surface adhesion [15] and membrane fouling [16, 17].

It is well known that the morphology and performance of the membranes depend largely on the conditions under which the membranes are prepared [18, 19]. The phase inversion method induced by immersion precipitation is the most common technique to develope asymmetric polymeric membranes [18, 20]. The immersion precipitation method involves mainly four steps, starting with the casting phase, then the evaporation stage followed by the gelation period, and finally the annealing step. Solvent evaporation is of importance in the case of the formation of the asymmetric structure that is the main property of the RO membrane [21].

In this study, the effect of evaporation time on resulting pore structure characteristics of both active and support layers were investigated by AFM analysis. Surface roughness parameters such as; roughness average (S_a), root mean square roughness (S_q), surface skewness (S_{sk}) and surface kurtosis (S_{ku}) values were obtained to compare the differences in the surface structures. The salt rejection performances of the membranes were also determined to relate them with the roughness parameters.

All roughness parameters can be calculated from the AFM image with an AFM software program. However, specific roughness parameters depend on the curvature on the membrane surface and also the size of the cantilever tip, as well as on the treatment of the captured images (plane correction, median fitler, *etc.*). Thus, the roughness parameters should not be considered as an absolute value that represents surface properties [2].

2. Experimental

2.1. Materials

Cellulose acetate was supplied by FLUKA, with a molecular weight of 37000 kg/kgmol and with a $\approx 40\%$ acetyl content used as a polymer. Both extra pure ($\approx 99\%$) acetone and formamide were supplied by MERCK, used as a solvent and swelling agent, respectively.

2.2. Preparation of CA Membranes

The immersion precipitation method was applied by following the steps of casting, evaporation, gelation, and annealing as described in the literature [22, 23].

Polymer solution, with a composition of 20 wt % CA, 69 wt % acetone and 11 wt % formamide was cast on a glass plate kept at the temperature of 263 K. After a varying period of solvent evaporation (15–130 s) in ambient atmosphere (the temperature of 298 K and relative humidity of 55–60 %), the membranes were immersed in a pure water bath (274 K) for gelation of the polymer solution for 90 min. Then the membranes were annealed in a water bath at 359 K for 6 min.

The film which was cast in the thickness of 300 μm by Doctor Blade reached the final thickness value of 131 ± 17.7 μm after drying.

2.3. Reverse Osmosis Tests

The laboratory set-up used in the permeation experiments was previously described [23].

The apparatus consists of a 30 l feed reservoir, test cell with an effective membrane area of 227 cm^2, a high pressure pump and hydraulic system. The salt rejection experiments were conducted at an operating pressure of $6 \cdot 10^3$ kPa.

The reverse osmosis performances of the prepared membranes were tested by using a feed with a concentration of 1 % NaCl by weight. The concentration of the Na$^+$ ion in both the feed and permeate were analyzed with Atomic Absorption Spectroscopy (Varian 10 Plus). The salt rejection performance was determined by the equation given below:

$$R = \left(1 - \frac{C_p}{C_F}\right) \cdot 100 \qquad (1)$$

where R is a rejection, %; C_p and C_F are Na$^+$ ion concentrations in the permeate and feed streams as ppm, respectively.

2.4. AFM Analysis

The surface structure of the membranes produced at several evaporation times, was observed by a multimode AFM (RT-SHPM) obtained from NanoMagnetic Instruments Co. The membrane surfaces were scanned by an aluminum reflex coated silicon probe (Tap 300AI, NanoMagnetics Instruments) having a spring constant of 40 N/m and a resonance frequency of 300 KHz in a tapping mode. The scan area and speed were chosen as 10x10 μm and 5 μm/s, respectively.

The membrane surfaces were compared in terms of roughness parameters such as; roughness average (S_a), root mean square roughness (S_q), surface skewness (S_{sk}) and surface kurtosis (S_{ku}).

Average roughness, S_a. The arithmetic average of the absolute values of the measured height deviations from the mean surface taken within the evaluation area. Analytically, it is given in Cartesian coordinates by [24]:

$$S_a = (1/Ae)\int_0^{L_y} \int_0^{L_x} |Z(x,y)| dx dy \qquad (2)$$

where Ae is the total area over which the values of the surface parameters are evaluated and $Z(x,y)$ is the *height function* which is used to represent the point-by-point deviations between the measured topography and the mean surface.

For a rectangular array of $M \times N$ digitized profile values Z_{jk}, the formula is given as:

$$S_a = \frac{1}{MN} \sum_{k=1}^{M} \sum_{j=1}^{N} |Z_{jk}| \qquad (3)$$

Root mean square (RMS) roughness, S_q. The root mean square average of the measured height deviations from the mean surface taken within the evaluation area. Analytically, S_q is given by:

$$S_q = \left((1/Ae)\int_0^{L_y} \int_0^{L_x} Z^2(x,y) dx dy\right)^{1/2} \qquad (4)$$

The digital approximation is:

$$S_q = \left[\frac{1}{MN} \sum_{k=1}^{M} \sum_{j=1}^{N} Z^2_{jk}\right]^{1/2} \qquad (5)$$

Surface skewness, Ssk. A measure of the asymmetry of surface heights about the mean surface.

Analytically, Ssk can be expressed as follows:

$$S_{sk} = \frac{1}{(S_q)^3 Ae}\int_0^{L_y} \int_0^{L_x} Z^3(x,y) dx dy \qquad (6)$$

For digitized profiles it can be calculated from:

$$S_{sk} = \frac{1}{(S_q)^3}\left[\frac{1}{MN} \sum_{k=1}^{M} \sum_{j=1}^{N} Z^3_{jk}\right] \qquad (7)$$

The surface skewness, related to the third momentum of the height distribution, informs about the asymmetry, that is, its dissimilarity relative to a Gaussian distribution. Surfaces with a positive skewness, such as turned surfaces have fairly high spikes that protrude above a flatter average. Surfaces with negative skewness, such as porous surfaces have fairly deep valleys in a smoother plateau. More random (for example, ground) surfaces have a skewness of about zero. A value of S_{sk} greater than about 1.5 in magnitude (positive or negative) indicates that the surface does not have a simple shape and more advanced parameters are needed to fully describe the surface structure [25].

Surface kurtosis, S_{ku}. A measure of the peakedness of the surface heights about the mean surface. Analytically, S_{ku} can be expressed as:

$$S_{ku} = \frac{1}{\left(S_q\right)^4 Ae} \int_0^{L_y} \int_0^{L_x} Z^4(x,y)dxdy \qquad (8)$$

For a digitized profile, it can be calculated by:

$$S_{ku} = \frac{1}{\left(S_q\right)^4} \left[\frac{1}{MN} \sum_{k=1}^{M} \sum_{j=1}^{N} Z_{jk}^4 \right] \qquad (9)$$

For the Gaussian distribution, the skewness is equal to zero and the kurtosis is equal to three.

In this study, surface roughness parameters were calculated from the AFM images using the built-in software SPM 1.16.13.1.

3. Results and Discussion

Identification (ID) of membranes having different evaporation times is given in the Table 1.

Table 1

IDs of membranes with their evaporation periods

Membrane ID	M1	M2	M3	M4	M5	M6
Evaporation time, s	15	25	70	90	110	130

3.1. Salt Rejection Performances

The salt rejection performance of membranes is given in Fig. 1 which helps to show the effect of the evaporation time on a membrane structure.

As the salt rejection of the membrane having 15 s of evaporation time, was so low (5.66 %), the active layer formation had not started yet. The salt rejection value increased to 30 % by using the membrane with 25 s of evaporation time. Although the salt rejection value of membrane M3 increased to a level of 56.23 %, it was not able to withstand higher pressures above $6 \cdot 10^3$ kPa due to the lack of mechanical strength. A well developed structure of the active layer was reached at 90 s of evaporation for the membrane M4. Both the development of the active layer formation and the salt rejection performance at 110 s of evaporation time (the membrane M5) reached their optimum levels. The decrease in the salt rejection of the membrane M6 can be explained by the distortion of the active layer.

3.2. AFM Analysis

AFM images taken from the active layer (top surface or air side) and support layer (bottom surface or glass side) of the asymmetric membranes produced at various evaporation times are presented in Figs. 2 and 3, respectively. As shown in the figures, the images have light and dark regions. The color intensity shows the vertical profile of the membrane surface, with light regions being the highest points and the dark points representing the depressions and pores.

Membranes are in an asymmetrical structure having a top thin skin layer (active) and a porous support layer. According to the kinetics of solvent evaporation time, structural changes develop in both layers.

When the images are compared, it can be seen that the active sides are much smoother than the support layer of the membrane. These differences are due to different natures of the air-solution and of the glass plate-solution interfaces. In the support layer of the membranes (Fig. 3) prepared using shorter evaporation times, the average size of the darker depression areas is higher than that for the membranes cast at longer evaporation times. The surface morphology also illustrated by the values of the statistical parameters (Table 2).
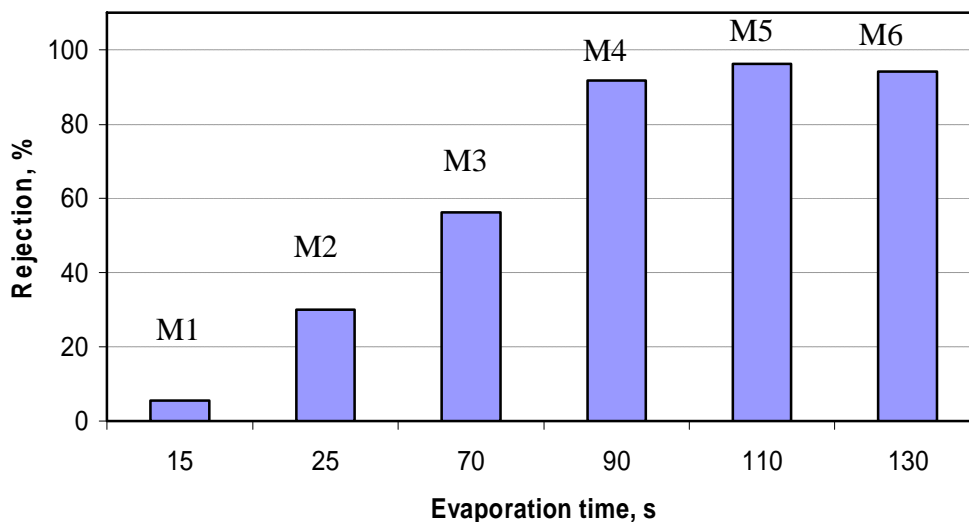

**Fig.1.** Comparison of the membranes performance prepared at various evaporation time

4. Conclusions

§ As evaporation time increases, pore diameters of both active and support layers of the membrane decrease. Salt rejection values increase up to 96 % by membranes having evaporation time of 110 s. Further extention of evaporation time results in a rejection loss.

§ Atomic force microscopy images indicated that an increase in evaporation time leads to a systematic decrease in pore size and an increase in surface roughness. Although roughness average (S_a) and root mean square roughness (S_q) values of the active layer increase with increasing evaporation time, there is no drastic change in roughness parameters (S_a, S_q) of support layers.

§ The negative values of skewness for active layer indicate the porous structure. Both active and support layers have kurtosis (S_{ku}) value scattering between 2.10–2.85.
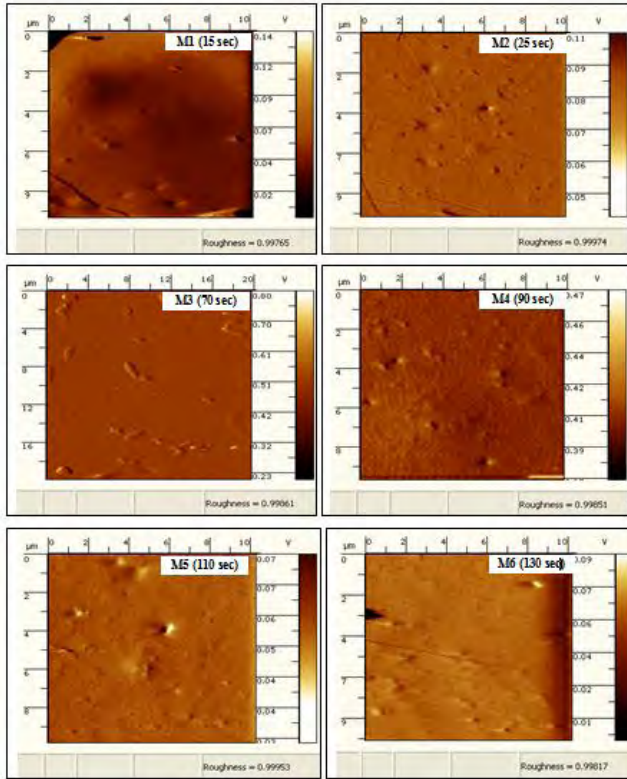
Fig. 2. AFM images of active layers of the membranes having the evaporation times of 15, 25, 70, 90, 110 and 130 s
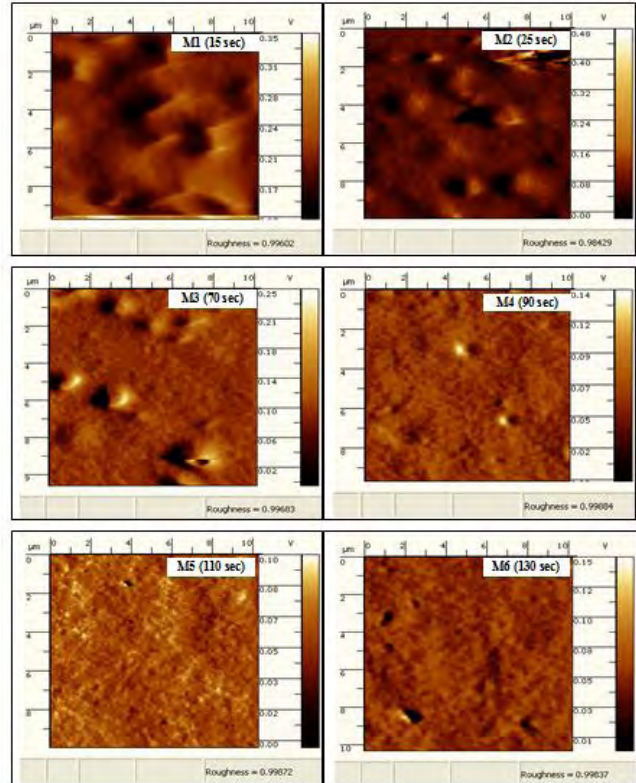
Fig. 3. AFM images of support layers of the membranes having the evaporation times of 15, 25, 70, 90, 110 and 130 s

Table 2

Roughness parameters of the membranes

	Membrane No	Evaporation time, s	Roughness average (S_a), nm	Root mean square (S_q), nm	Surface skewness (S_{sk}), nm	Surface kurtosis, (S_{ku}), nm
Active layer	M1	15	217.75	272.10	-1.41	2.83
	M2	25	203.54	239.13	-0.18	2.17
	M3	70	335.31	417.72	-0.84	2.10
	M4	90	434.48	497.85	-0.24	2.12
	M5	110	571.23	655.56	-0.66	2.76
	M6	130	753.68	849.47	-1.14	2.58
Support layer	M1	15	202.30	245.45	0.18	2.53
	M2	25	256.80	306.50	0.31	2.10
	M3	70	261.52	295.81	0.19	2.71
	M4	90	238.95	276.67	0.20	2.85
	M5	110	334.48	397.85	0.24	2.12
	M6	130	349.14	416.13	0.45	2.19

Acknowledgements

References

[1] Stamatialis D., Dias C. and Pinho M.: J. Membr. Sci., 1999, **160**, 235.

[2] Khulbe K., Feng C. and Matsuura T.: Synthetic Polymeric Membranes: Characterization by Atomic Force Microscopy, Springer 2008.

[3] Yoshida W. and Cohen Y.: J. Membr. Sci., 2003, **215**, 249.

[4] Bowen W., Hilal N., Lovitt R. and Williams P.: J. Colloid Interface Sci., 1996, **180**, 350.

[5] Bowen W., Hilal N., Lovitt R. and Williams P.: J. Membr. Sci., 1996, **110**, 229.

[6] Bowen W. and Doneva T.: Desalination, 2000, **129**, 163.

[7] Bessieres A., Meireles M., Coratger R. *et al.*: J. Membr. Sci., 1996, **109**, 271.

[8] Singh S., Khulbe K., Matsuura T. and Ramamurthy P.: J. Membr. Sci., 1998, **142**, 111.

[9] Ochoa N., Pradanos P., Palacio L. *et al.*: J. Membr. Sci., 2001, **187**, 227.

[10] Hilal N., AI-Zoubi H., Darwish N. and Mohammad A.: Desalination, 2005, **177**, 187.

[11] Tan J. and Matsuura T.: J. Membr. Sci., 1999, **160**, 7.

[12] Al-Jeshi S. and Neville A.: Desalination, 2006, **189**, 221.

[13] Hirose M., Ito H. and Kamiyama Y.: J. Membr. Sci., 1996, **121**, 209.

[14] Madaeni S.: Desalination, 2001, **139**, 371.

[15] Bowen W., Hilal N., Lovitt R. and Wright C.: J. Membr. Sci., 1998, **139**, 269.

[16] Vrijenhoek E., Hong S. and Elimelech M.: J. Membr. Sci., 2001, **188**, 115.

[17] Bowen W. and Doneva T.: J. Colloid Interface Sci. 2000, **229**, 544.

[18] Mulder M.: Basic Principles of Membrane Technology, Kluwer Academic Publishers, Dordrecht 1997.

[19] Mohammadi T. and Saljoughi E.: Desalination, 2009, **243**, 1.

[20] Kesting R.: Synthetic Polymeric Membranes, 2nd edn. Wiley&Sons, New York 1985.

[21] Paulsen F., Shojaie S. and Krantz W.: J. Membr. Sci., 1994, **91**, 265.

[22] Kezin R.: MSc. thesis, Ege University, Turkey 2006.

[23] Baser A.: MSc. Dissertation, Ege University, Turkey 2006.

[24] An American National Standard ASME B46.1-2002, Surface Texture (surface roughness, waviness, and lay), American Society of Mechanical Engineers, U.S.A., 2003.

[25] Mendez-Vilas A., Bruque J. and Gonzalez-Martın M.: Ultramicroscopy, 2007, **107**, 617.

МОРФОЛОГІЧНА ХАРАКТЕРИСТИКА МЕМБРАН ЗВОРОТНОГО ОСМОСУ НА ОСНОВІ АЦЕТАТУ ЦЕЛЮЛОЗИ МЕТОДОМ АТОМНО-СИЛОВОЇ МІКРОСКОПІЇ (АСМ) – ВПЛИВ ЧАСУ ВИПАРОВУВАННЯ

Анотація. За допомогою атомно-силової мікроскопії (АСМ) досліджено структуру поверхні асиметричних мембран з ацетату целюлози приготовлених методом фазової інверсії. Відмінності в морфології поверхні були виражені чотирма типами параметрів шорсткості, таких як: середня шорсткість (S_a), середньоквадратична шорсткість (S_q), поверхнева асиметрія (S_{sk}) та поверхневий ексцес (розподіл) (S_{ku}). Встановлено взаємозв'язок між шорсткістю та видаленням солі. Показано, що збільшення часу випаровування призводить до зміни морфології мембран і ефективності.

Ключові слова: атомно-силова мікроскопія, мембрана зворотного осмосу, морфологія, шорсткість поверхні.